ELSEVIER

Thermochimica Acta 266 (1995) 189–202

thermochimica
acta

# High-pressure DTA study on liquid crystalline polyesters with biphenyl as mesogen [☆]

Yoji Maeda [a,*], Toshio Mabuchi [b], Junji Watanabe [b]

[a] *National Institute of Materials and Chemical Research, 1-1 Higashi, Tsukuba, Ibaraki 305, Japan*
[b] *Department of Polymer Chemistry, Tokyo Institute of Technology, Ookayama, Meguro-ku, Tokyo 152, Japan*

---

## Abstract

The phase transition of a homologous series of liquid crystalline polyesters was studied under hydrostatic pressures up to 300 MPa by using a high-pressure DTA apparatus. The thermotropic polyesters, abbreviated as PB-*n* (where *n* is an even number of methylene units), were prepared from 4,4′-dihydroxybiphenyl and aliphatic dibasic acids containing an even number of methylene groups from 8 to 22 units. The $T$ vs. $P$ phase diagrams of the PB-10, PB-12, PB-14 and PB-18 polyesters were constructed. PB-10 shows a simple phase transition of crystal (K)–smectic-H ($S_H$)–isotropic melt (I) over the whole pressure region. PB-12 shows a similar K–$S_H$–I transition in the low-pressure region below about 100 MPa. At high pressures above 100–120 MPa, however, PB-12 exhibits a $T$ vs. $P$ relation that is different from that in the low-pressure region. The phase diagram supports the existence of the pressure-induced smectic phase which was assigned to be the smectic-B ($S_B$) phase. The PB-14, PB-16, and PB-18 samples show an additional first-order transition just below the K–$S_H$ transition at atmospheric pressure. The new transition peak increases with increasing space *n* in the PB-*n* samples, in contrast to the decrease in the K–$S_H$ transition peak. The transition is a kind of crystal transition between the low- and high-temperature phases, denoted here as $K_1$ and $K_2$. The thermal behavior of these samples can be understood as enantiotropic transitions through the $K_1$–$K_2$–$S_H$–I route. They show the same type of $T$ vs. $P$ phase diagram, indicating the $K_1$–$K_2$, $K_2$–$S_H$ and $S_H$–I transition lines. The phase diagrams indicate that the stable region of the $S_H$ phase broadens with increasing pressure. However, the $K_2$–$S_H$ transition peak becomes too small to be detected under pressures of 300–400 MPa.

*Keywords:* Crystal–crystal transition; Crystal–smectic transition; High-pressure DTA; Phase diagram; Thermotropic polyesters

---

* Corresponding author.

[☆] Dedicated to Hiroshi Suga on the Occasion of his 65th Birthday.

*SSDI* 0040-6031(95)02439-5

## 1. Introduction

Semiflexible homopolyesters having rigid and flexible segments in the repeating unit are attractive because their transition temperatures can be controlled by varying the number of methylene units in the flexible segment [1–3]. Although much interest has been given to polymers forming thermotropic mesophases, there are only a few studies on the thermal behavior of thermotropic polyesters under hydrostatic pressures. Samulski and coworkers [4,5] reported two interesting pressure effects, a pressure-induced crystal habit and a pressure-induced mesophase, of the aromatic copolyester HIQ-20, composed of 20% hydroxybenzoic acid, 40% isophthalic acid and 40% hydroquinone. Maeda and coworkers [6,7] studied the effect of pressure on the structure and thermal properties of a main-chain thermotropic polyester in which crystalline polymorphs are found under pressure.

Asrar et al. [8] reported the synthesis and properties of a homologous series of 4,4′-dihydroxybiphenyl-alkanedioic acid polyesters, prepared from 4,4′-dihydroxy-biphenyl as mesogen and aliphatic dibasic acids containing 5–12 methylene units as flexible spacer. The polyesters are abbreviated as PB-*n*, *n* indicating the number of methylene units in the flexible spacer. The chemical structure of the PB-*n* polyester is

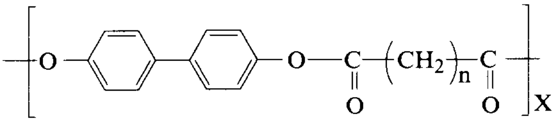

The structure–property relationship of the PB-*n* polyesters has been studied at atmospheric pressure [9]. The thermotropic polyesters are known to exhibit a unique odd–even effect. The PB-*n* samples formed from dibasic acids with an odd number of methylene units exhibit a nematic phase, while those having an even number show a smectic mesophase. Polyesters with even *n* numbers show the smectic-H ($S_H$) phase over a relatively broad temperature region between the crystalline solid and the isotropic melt. The $S_H$ phase is identified as a tilted smectic phase [10]. We have reported the thermal behavior and phase diagram of the PB-7 and PB-8 polyesters under hydrostatic pressures [11]. Typical transitions of crystal (K)–nematic (N)–isotropic melt (I) for PB-7, and K–$S_H$–I for PB-8 were clearly observed at pressures up to 300 MPa, respectively.

Smectic liquid crystals are interesting because significant pressure effects might be expected as a result of the alternate arrangement of rigid mesogenic core and flexible aliphatic spacer in the repeating unit. We have reported the pressure-induced mesomorphism of the PB-12 polyester using wide-angle X-ray scattering (WAXS) under hydrostatic pressures [12]. The usual $S_H$ phase in the low-pressure region below 90–100 MPa is transformed to the smectic-B ($S_B$) phase at higher pressures. The phase diagram constructed from the high-pressure X-ray diffraction study clearly indicates the existence of stable phases of the K, $S_H$, $S_B$, and I phases.

In this study, the thermal behavior of four homologous samples of the thermotropic polyesters PB-10, PB-12, PB-14 and PB-18 was investigated using a high-pressure DTA apparatus [13,14]. Characterization of the samples was performed using DSC and wide-angle X-ray scattering at atmospheric pressure.

## 2. Experimental

### 2.1. Characterization

The synthesis of the PB-*n* polyesters used in this study is described elsewhere [8, 9]. Polyesters were synthesized by melt condensation (trans-esterification) of 4,4′-dihydroxybiphenyl and aliphatic dibasic acids at about 523 K and by interfacial polycondensation. The inherent viscosities of the samples were determined by an Ubbelhode viscometer at 298 K using 0.5 g dl$^{-1}$ solution in a 60/40 mixture by weight of phenol and tetrachloroethane. The inherent viscosities of PB-10, PB-12 and PB-14 were 0.65, 0.60 and 0.72 dl g$^{-1}$, respectively. The viscosities of the samples from PB-16 to PB-22 could not be measured because of low solubility in the mixed solvent, but they are taken to have the same level of inherent viscosity. DSC measurements were performed at a scanning rate of 10 K min$^{-1}$ using a Perkin-Elmer DSC-II differential scanning calorimeter. The DSC samples weighed about 3–5 mg. The temperature and heat of fusion were calibrated with In standard.

### 2.2. High-pressure DTA measurements

The thermal behavior under pressure of the PB-*n* polyesters was measured at hydrostatic pressures up to 400 MPa using the high-pressure DTA apparatus reported previously [13, 14]. The sample, inside a platinum cup with an inner diameter of 3 mm and depth of 2 mm, was coated with epoxy adhesive to fix the sample at the bottom of the platinum cup and, at the same time, to inhibit direct contact with the silicone oil pressure medium. Dimethylsilicone oil, with a viscosity of 100 centistokes, was used as the pressure medium. The temperature was measured with a precision of ± 0.1 K by C–A thermocouples. The DTA measurements of the polyester, 3–5 mg in weight, were performed at a constant heating rate of 5 K min$^{-1}$ under hydrostatic pressure. Transition temperatures were determined as the top of the peaks on both the DSC and high-pressure DTA curves.

## 3. Results and discussion

Fig. 1 shows the DSC heating curves of a homologous series of PB-*n* samples. The PB-10 sample clearly shows two endothermic peaks indicating the K–$S_H$ and $S_H$–I transitions, respectively. This is entirely the same thermal behavior as that of PB-8, as reported previously [11]. However, all the samples between PB-14 and PB-20 show an additional broad peak at temperatures just below the usual K–$S_H$ transition. The new transition peak becomes more clear with longer flexible spacers in the PB-*n* sample, while the K–$S_H$ transition becomes lower. The former transition may be a kind of crystal transition. The low- and high-temperature crystal phases are labeled here as $K_1$ and $K_2$, respectively. The phase transition of $K_1$–$K_2$–$S_H$–I occurs enantiotropically at atmospheric pressure. As can be seen in Fig. 1, these transition peaks shift to low temperatures in PB-*n* samples with longer spacer lengths.

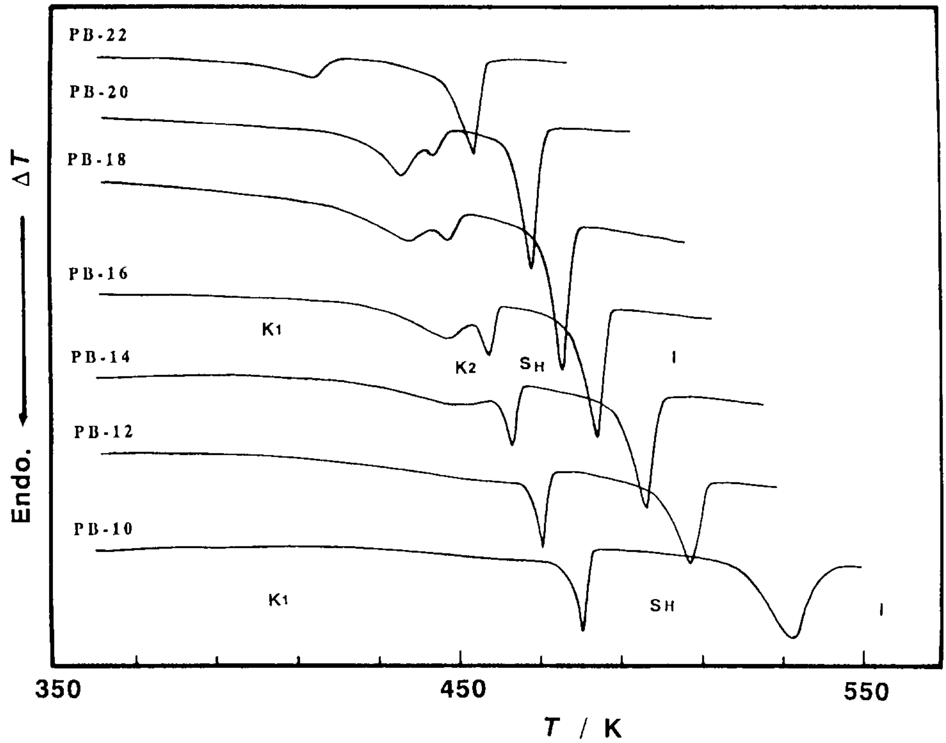

Fig. 1. DSC heating curves of the homologous series of PB-*n* polyesters. Heating rate, 10 K $\mathrm{min}^{-1}$.

Fig. 2 shows the relation between the transition temperatures and the number *n* of methylene units in the flexible spacer of the PB-*n* polyesters. It can be seen that both linear relations, the $T_{\mathrm{K-SH}}$ vs. *n* and $T_{\mathrm{SH-I}}$ vs. *n* curves, show a distinct change in slope at $n = 12$. The reason for this is not clear at present, but the experimental results do indicate that the thermal behavior is separated into two categories. The PB-8 and PB-10 samples clearly show a simple phase transition of the type $\mathrm{K} \leftrightarrow \mathrm{S_H} \leftrightarrow \mathrm{I}$. However, PB-*n* samples with $n > 14$ show some complex transitions between the $K_1$ and $S_H$ phases because an additional $K_1$–$K_2$ transition is clearly observed. Table 1 lists the experimental data for the transition temperature and transition enthalpy (in kJ $\mathrm{mol}^{-1}$, where "mol" refers to a repeating unit).

Typical WAXS pattern of these crystals show a sharp low-angle reflection at around $2\theta = 3$–4° and two strong wide-angle reflections at about 20° [9]. The low-angle reflection indicates the molecular length of PB-*n* repeating unit in the chain direction. The *d* spacings of the $K_1$, $K_2$ and $S_H$ phases were estimated from the observed WAXS patterns of the homologous series of PB-*n* polyesters. Fig. 3 shows the relation between the *d* spacing of the $K_1$, $K_2$, and $S_H$ phases and the number of methylene units in the spacer *n*. A linear relation is held for each phase of the $K_1$, $K_2$ and $S_H$ phases. It can be

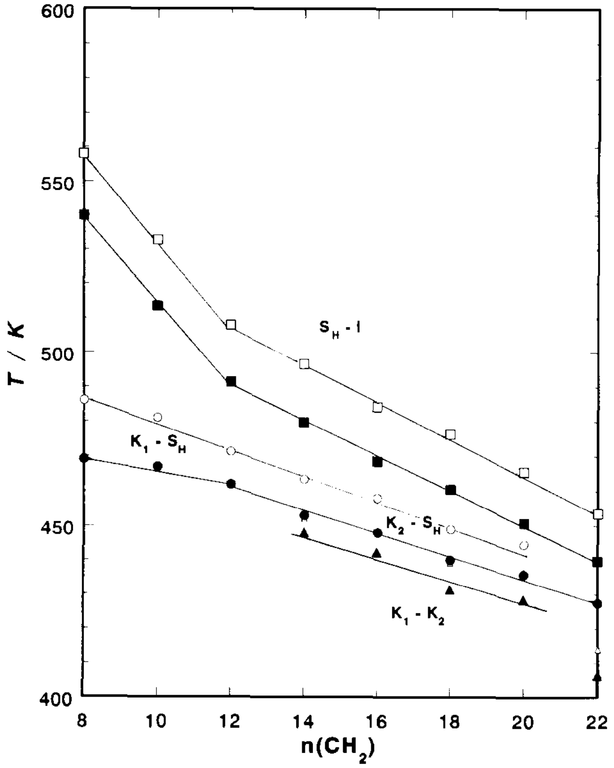

Fig. 2. Relation of the transition temperatures to the numbers *n* of methylene units in the flexible spacer of a series of PB-*n* polyesters: ▲, $K_1$–$K_2$ transition; ●, $K_1$–$S_H$ and $K_2$–$S_H$ transitions; and ■, $S_H$–I transition. Open and solid symbols are for data from heating and cooling processes, respectively.

Table 1
Thermodynamic data of the phase transitions of the PB-*n* polyesters

| Sample | $K_1$–$K_2$ transition | | $K_2$–$S_H$ transition | | $S_H$–I transition | |
|---|---|---|---|---|---|---|
| | *T*/K | Δ*H*/kJ mol$^{-1}$ | *T*/K | Δ*H*/kJ mol$^{-1}$ | *T*/K | Δ*H*/kJ mol$^{-1}$ |
| PB-8 | | | 486.1 | 12.7 | 558.1 | 18.3 |
| PB-10 | | | 481.2 | 14.8 | 532.7 | 22.1 |
| PB-12 | | | 471.3 | 15.8[a] | 507.9 | 18.2 |
| PB-14 | 452.0 | 18.9[a] | 463.4 | yes | 496.6 | 23.8 |
| PB-16 | 448.1 | 22.1[a] | 458.0 | yes | 484.3 | 24.6 |
| PB-18 | 439.2 | 19.5[a] | 449.0 | yes | 476.3 | 25.9 |
| PB-20 | 436.5 | 25.4[a] | 444.6 | yes | 465.5 | 28.3 |
| PB-22 | 414.2 | 18.0[a] | | yes | 453.6 | 34.4 |

[a] Total enthalpy change of the double peaks of the $K_1$–$K_2$ and $K_2$–$S_H$ transitions.

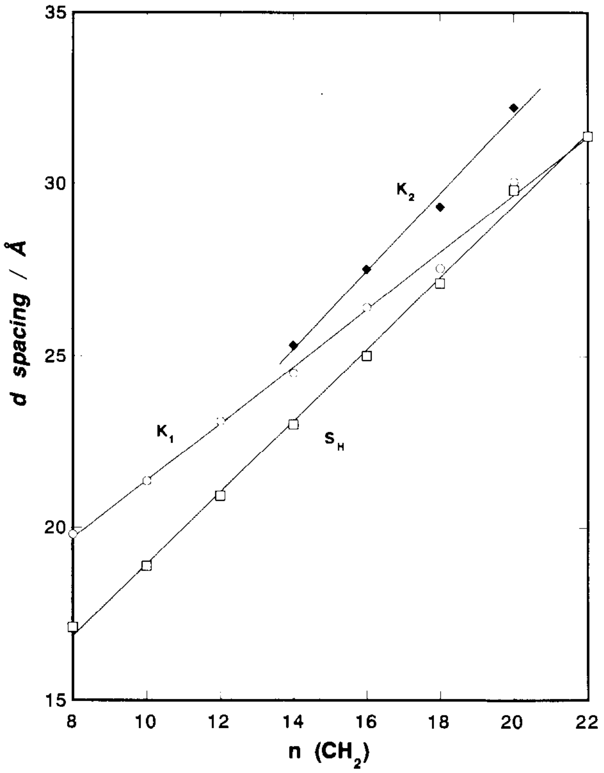

Fig. 3. Relation of $d$ spacing in the molecular chain direction to the number $n$ of the methylene units in the flexible spacer of the PB-$n$ samples: ○, $K_1$, low-temperature crystal phase; ◆, $K_2$, high-temperature phase; and □, $S_H$, smectic-H phase.

seen that the $K_1$–$n$ line merges with the $S_H$–$n$ line at about $n = 22$, and that the $K_2$–$n$ line is located between $n = 14$ and $n = 20$. If the $K_2$–$n$ line is extrapolated to small $n$, it would cross the $K_1$–$n$ line at about $n = 12$. This structural information corresponds well with the DSC thermal behavior: the $K_1$–$K_2$ transition peak clearly appears in the PB-14, PB-16 and PB-18 samples. The experimental results of the series of PB-$n$ polyesters indicate overwhelmingly that there is little dependence of the thermal and structural behavior upon the variance in inherent viscosity of the PB-$n$ samples because they have the same order of inherent viscosity.

The high-pressure DTA measurements of the PB-$n$ samples were performed at hydrostatic pressures up to 300 MPa. The PB-10 polyester shows the typical DTA pattern of the sharp $K_1$–$S_H$ and $S_H$–I transition peaks over the whole pressure region. Fig. 4 shows the $T$ vs. $P$ phase diagram of the PB-10 sample. Both the $K_1$–$S_H$ and $S_H$–I lines change almost linearly with pressure. It is common in liquid crystals that the positive slope, $\mathrm{d}T/\mathrm{d}P$, of the $S_H$–I line is much greater than that of the $K_1$–$S_H$ line. This means that the thermal stability of the $S_H$ phase is enhanced at high pressure. Fig. 5

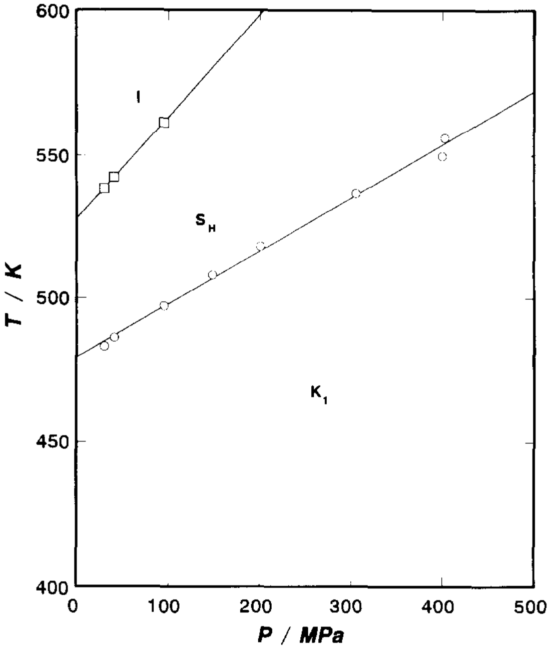

Fig. 4. $T$ vs. $P$ phase diagram of the PB-10 polyester: ○, K–$S_H$ transition; and □, $S_H$–I transition.

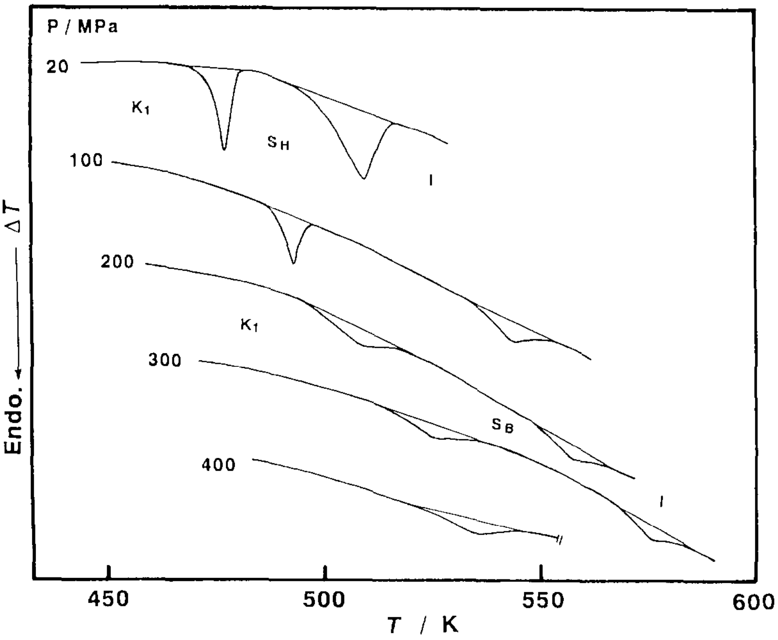

Fig. 5. High-pressure DTA curves of the PB-12 polyester with an inherent viscosity of $[\eta] = 0.60$. Heating rate, 5 K $\text{min}^{-1}$.

shows the DTA curves of the PB-12 sample on heating at various pressures. In the low-pressure region below 100 MPa, the DTA curves show the same pattern as the PB-10 sample. The thermal behavior completely corresponds with the WAXS data reported previously [12]. With increasing pressure above about 200 MPa, however, the sharp peak of the $K_1$–$S_H$ transition becomes broad and small. The peak temperatures of the K–S and S–I transitions are plotted in Fig. 6 as a function of pressure. The transition lines are almost linear with pressures up to 100–150 MPa. Fig. 6 shows clearly that the $K_1$–$S_H$ line changes its slope at about 150 MPa, while the $S_H$–I line changes its linear slope at around 100 MPa. The inflection in the $K_1$–$S_H$ and $S_H$–I transition lines is due to the appearance of the pressure-induced smectic-B ($S_B$) phase at pressures above 100–120 MPa [12]. The $T$ vs. $P$ phase diagram in Fig. 6 corresponds well with the diagram constructed by the X-ray measurements [15]. Another sample of PB-12 with an inherent viscosity of $[\eta] = 0.75$ showed a very curious thermal behavior. Figs. 7 and 8 show the DTA heating curves and the phase diagram of the PB-12 sample at pressures up to 300 MPa. Also in this sample, the $S_H$ and $S_B$ phases are observed in the low- and high-pressure regions, respectively. It is interesting to note that in Fig. 7 an additional broad peak appears overlapped with the typical K–$S_H$ transition peak at pressures above about 100 MPa, while the latter peak becomes small with increasing pressure. The reason why the additional peak cannot be seen in the PB-12 sample with $[\eta] = 0.60$ but can be seen in the sample with $[\eta] = 0.75$, is not clear. However, such double peaks in the K–$S_H$ transition region are common in the PB-14, PB-16, PB-18

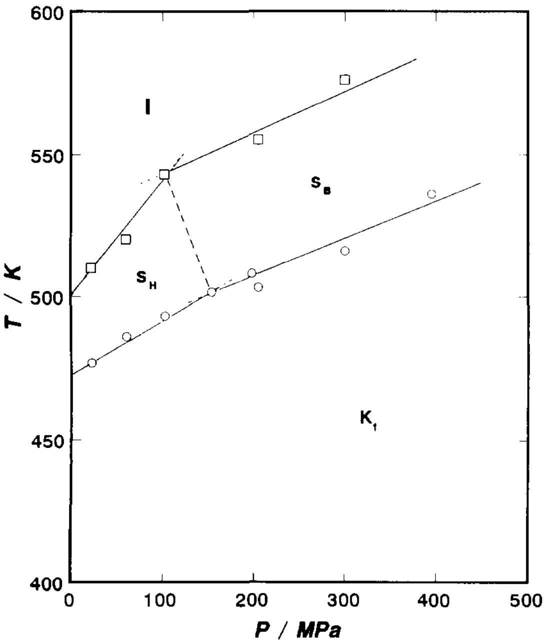

Fig. 6. $T$ vs. $P$ phase diagram of the PB-12 sample.

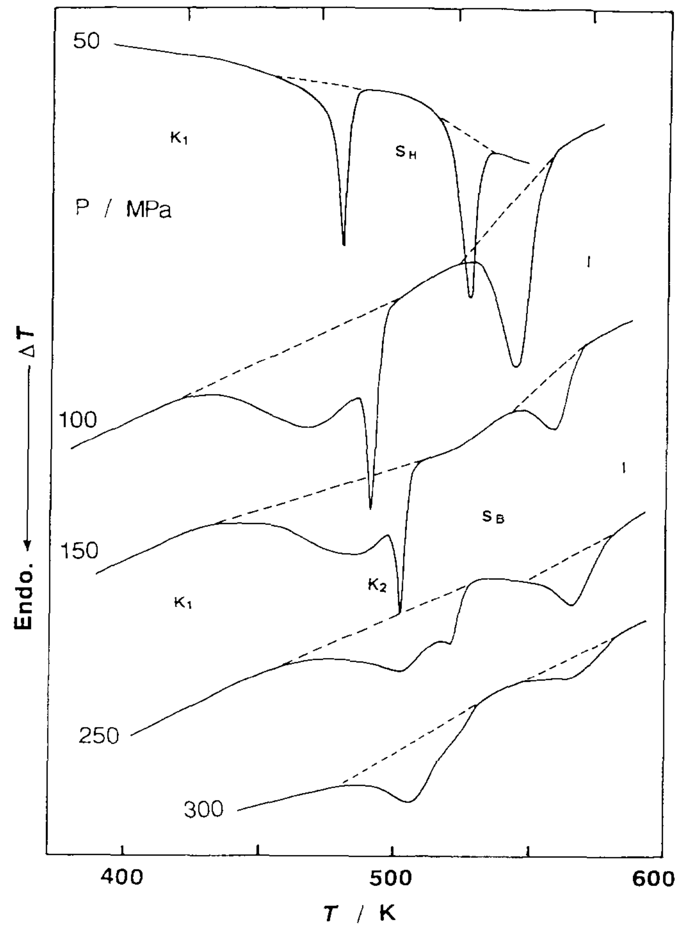

Fig. 7. DTA curves of another PB-12 sample with an inherent viscosity of $[\eta] = 0.75$.

and PB-20 samples as shown in Fig. 1. The curious thermal behavior of the PB-12 sample with an inherent viscosity of $[\eta] = 0.75$ may be due to the formation of a pressure-induced high-temperature crystal phase in addition to the $S_B$ phase under high pressures. Accordingly, the thermal behavior can be understood if the $K_1$–$K_2$ and $K_2$–$S_B$ transitions are considered to occur consecutively on heating at pressures above 100 MPa.

Fig. 9 shows the DTA heating curves of PB-14 polyester at various pressures. The DTA curves at 50 and 100 MPa show the same thermal behavior as one of the DSC curves in Fig. 1: broad $K_1$–$K_2$ peak, sharp $K_2$–$S_H$ peak, and $S_H$–I peak at the highest temperature. The $K_2$–$S_H$ transition peak becomes small with increasing pressure above 200 MPa and then disappears at about 400–450 MPa. Fig. 10 shows the $T$ vs. $P$ phase diagram of the PB-14 sample. The $K_1$–$K_2$ and $K_2$–$S_H$ transition lines have almost the

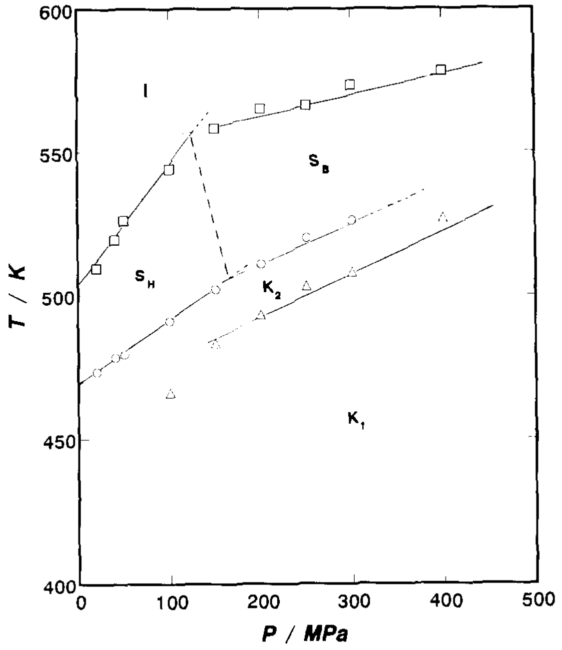

Fig. 8. *T* vs. *P* phase diagram of another PB-12 sample.

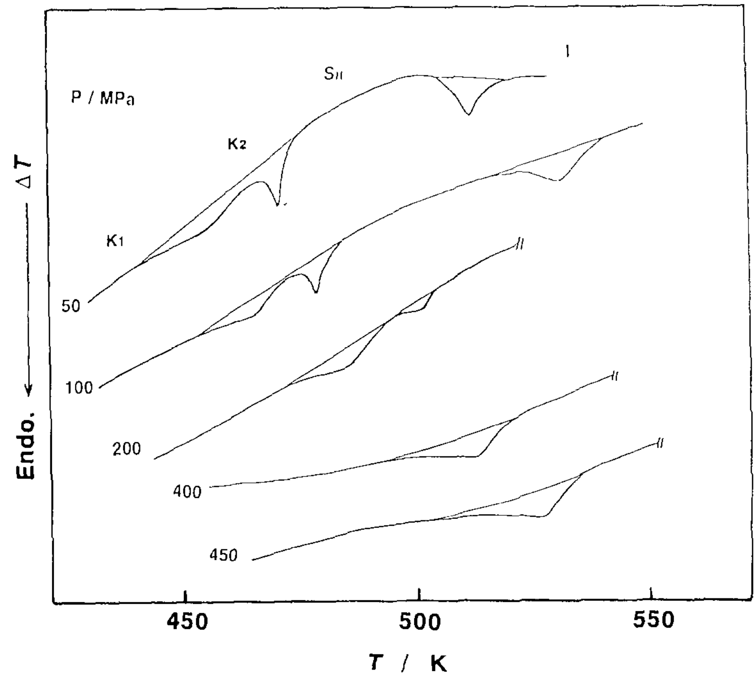

Fig. 9. High-pressure DTA curves of the PB-14 polyester. Heating rate, 5 K min$^{-1}$.

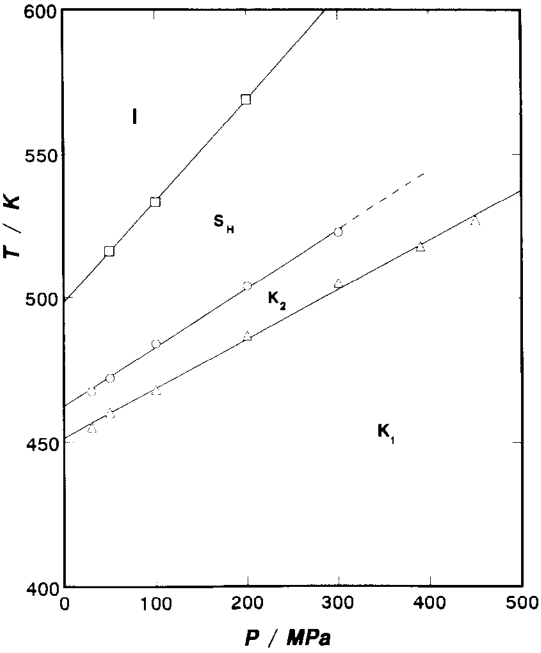

Fig. 10. T. vs. P phase diagram of the PB-14 sample: △, $K_1$–$K_2$ transition; ○, $K_2$–$S_H$ transition; and □, $S_H$–I transition.

same slopes, but the latter is ambiguous at higher pressures. Such a strange phenomenon can also be observed in the PB-18 sample. Fig. 11 shows the DTA heating curves of the PB-18 polyester at pressures up to 300 MPa. As can be seen, the double peaks of the $K_1$–$K_2$ and $K_2$–$S_H$ transitions are observed as the main and shoulder peaks, respectively, of the K–S transition region. The sharp but small $K_2$–$S_H$ peak decreases with increasing pressure and it is ambiguous at pressures above about 300 MPa. Fig. 12 shows the T vs. P phase diagram of the PB-18 sample. Like the transition lines in the PB-14 sample, the $K_2$–$S_H$ transition line is almost parallel with the $K_1$–$K_2$ line over the whole pressure region.

Table 2 lists the approximate equations of the first-order polynomial in pressure for the samples ranging from PB-10 to PB-18. The K–$S_H$ transition lines are almost parallel in all the PB-*n* samples. It is common in PB-*n* samples with $n > 14$ that the $K_2$–$S_H$ transition peak becomes ambiguous at higher pressures. The possibility that the smectic mesophase might disappear at high pressure is inconsistent with the phase diagrams in Figs. 10 and 12 which show a broadening in the temperature region of the stable $S_H$ phase at high pressures. So it is reasonable to consider that the $K_2$–$S_H$ transition of the PB-14 and PB-18 samples occurs as a subtle change under such high pressures because the PB-*n* crystals with longer methylene units seem to be deformed significantly in the molecular chain direction by hydrostatic pressure. X-ray and NMR characterization of the crystalline and smectic phases of the PB-*n* ($n > 14$) polyesters

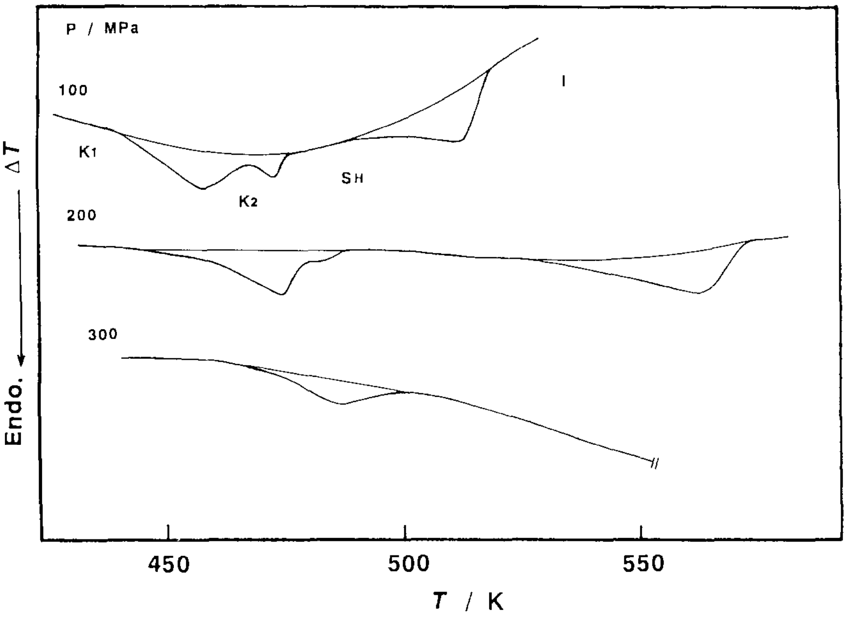

Fig. 11. High-pressure DTA curves of the PB-18 polyester. Heating rate, 5 K min$^{-1}$.

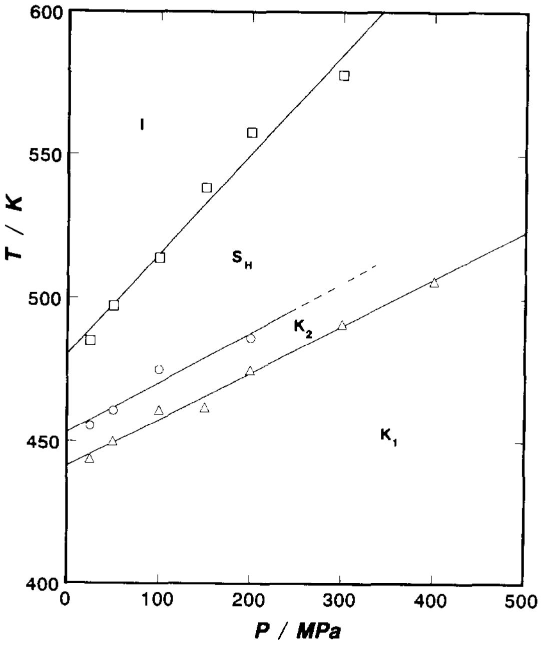

Fig. 12. T vs. P phase diagram of the PB-18 sample.

Table 2
Approximate expression, $T = A + BP$, for the $K_1$–$K_2$, $K_2$–$S_H$ and $S_H$–I transitions of the PB-*n* ($n = 10$–18) polyesters

| Sample | $K_1$–$S_H$ transition | | $S_H$–I transition |
|---|---|---|---|
| PB-8 | $T = 488.0 + 0.204P$ | | $T = 549.2 + 0.360p$ |
| PB-10 | $T = 479.3 + 0.186P$ | | $T = 527.7 + 0.353P$ |
| PB-12 | | $0.1\,\text{MPa} \leq P \leq 100\,\text{MPa}$ | |
| | $T = 468.7 + 0.223P$ | | $T = 502.7 + 0.424P$ |
| | | $P \geq 100$–$120\,\text{MPa}$ | |
| | ($K_1$–$S_B$ transition)<br>$T = 475.0 + 0.176P$ | | ($S_B$–I transition)<br>$T = 539.8 + 0.105P$ |
| | $K_1$–$K_2$ transition | $K_2$–$S_H$ transition | $S_H$–I transition |
| PB-14 | $T = 451.4 + 0.172P$ | $T = 462.3 + 0.205P$ | $T = 498.2 + 0.354P$ |
| PB-18 | $T = 441.3 + 0.164P$ | $T = 453.2 + 0.174P$ | $T = 480.5 + 0.348P$ |

would clarify the structures of the $K_1$, $K_2$, and $S_H$ phases and the transformation mechanism of the $K_1$–$K_2$ and $K_2$–$S_H$ transitions under atmospheric and hydrostatic pressures.

## 4. Conclusion

The thermal behavior of four homologous thermotropic polyesters, PB-10, PB-12, PB-14 and PB-18, with an alternate arrangement of 4,4′-dihydroxybiphenyl as mesogen and alkanedioic acid as a flexible spacer in the repeating unit was studied under hydrostatic pressures up to 300 MPa using a high-pressure DTA apparatus. The PB-10 polyester shows a simple phase transition, crystal ($K_1$)–smectic–H ($S_H$)–isotropic (I), over the whole pressure region. The PB-12 polyester shows the typical $K_1$–$S_H$–I phase transition in the low-pressure region below about 100 MPa. At high pressures above 100–150 MPa, however, both the $K_1$–$S_H$ and $S_H$–I transition lines change to the $K_1$–$S_B$ and $S_B$–I transition lines, indicating the appearance of the pressure-induced smectic-B ($S_B$) phase at high pressures. The $T$ vs. $P$ phase diagram suggesting the appearance of the $S_B$ phase at high pressures is consistent with the phase diagram constructed from the X-ray measurements under pressure [12, 15]. The PB-14 and PB-18 polyesters show an additional $K_1$–$K_2$ transition just below the typical K–$S_H$ transition. In these polyesters, the $K_1$–$K_2$–$S_H$–I transition is clearly observed at pressures up to about 200 MPa. However, the DTA peak of the $K_2$–$S_H$ transition becomes ambiguous with increasing pressure and then is undetectable at about 300–400 MPa. This may be reduced to the hydrostatic compression of both crystals, especially the $K_2$ crystals, of the PB-*n* polyesters with longer flexible spacers including aliphatic methylene units. The structural change during the $K_2$–$S_H$ transition might induce ambiguous DTA thermal behavior in the thermotropic PB-*n* polyesters.

## Acknowledgement

We acknowledge Dr. M. Sone for the measurement of the inherent viscosity of the series of PB-*n* polyesters.

## References

[1] A. Roviello and A. Sirigu, Makromol. Chem., 183 (1982) 895.
[2] A.C. Griffin and S.J. Havens, Mol. Cryst. Liq. Cryst. Lett., 49 (1979) 239.
[3] L. Strzelecki and D. van Luyen, Eur. Polym. J., 16 (1980) 303.
[4] E.T. Samulski, B.S. Hsiao and M.T. Shaw, Macromolecules, 21 (1988) 543.
[5] E.T. Samulski, B.S. Hsiao and M.T. Shaw, J. Polym. Sci. Polym. Phys. Ed., 28 (1990) 189.
[6] Y. Maeda and A. Blumstein, Mol. Cryst. Liq. Cryst., 195 (1991) 169.
[7] Y. Maeda, N. Tanigaki and A. Blumstein, Mol. Cryst. Liq. Cryst., 237 (1993) 407.
[8] J. Asrar, H. Toriumi, J. Watanabe, W.R. Krigbaum and A. Cierri, J. Polym. Sci. Polym. Phys. Ed., 21 (1983) 1119.
[9] W.R. Krigbaum, J. Watanabe and T. Ishikawa, Macromolecules, 16 (1983) 1271.
[10] J. Watnabe and W.R. Krigbaum, Macromolecules, 17 (1984) 2288.
[11] Y. Maeda and H. Toriumi, Makromol. Chem., 194 (1993) 3123.
[12] Y. Maeda and J. Watanabe, Macromolecules, 26 (1993) 401.
[13] Y. Maeda and H. Kanetsuna, Bull. Res. Inst. Polym. Text., 149 (1985) 119.
[14] Y. Maeda, Thermochim. Acta, 163 (1990) 211.
[15] Y. Maeda and J. Watanabe, Macromolecules, 28 (1995) 1661.